Pile Group Interaction Based on Field Monitoring and Load Tests

K. Yamashita[1], S. Wakai[1], J. Hamada[1] and T. Tanikawa[1]
[1]*Takenaka Research and Development Institute, Takenaka Corporation, Chiba, Japan*
Email: yamashita.kiyoshi@takenaka.co.jp

ABSTRACT: The effects of pile group interaction on settlements were investigated based on the results of two monitoring cases of piled raft foundations and single pile load tests in soft ground. The first case was a piled raft consisting piles embedded in deep dense sand with large spacing supporting a 12-story building, and the case second was a piled raft consisting of friction piles with large spacing supporting a 7-story building. The load-settlement data of the monitored and test piles of different dimensions were compared using a modification factor derived from an elastic solution for the axial response of a single pile. Based on the investigation, it was found that the modified load-settlement data of the monitored piles were generally consistent with the static load-settlement curve of a single pile. Therefore, no significant effects of pile group interaction on settlement were found. In such cases as pile groups with large spacing, single pile load test data can be more useful in the settlement prediction of piled rafts and pile groups. In addition, it was found that the pile head stiffness of the equivalent static load-settlement curve derived from the rapid load testing in clay soils using the UPM was considerably large compared to the stiffness of the static load test curve, as pointed out by previous studies.

KEYWORDS: Piled raft foundation, Field monitoring, Static load test, Rapid pile load testing, Effects of group interaction, Rate effects

1. INTRODUCTION

Piled raft foundations have been used in many countries mainly as building foundations, and the settlement and the load sharing between raft and piles have been carefully investigated for the selected buildings (Katzenbach et al., 2000; Yamashita et al. 2011a; Yamashita et al. 2011b). Recently, case histories of monitoring seismic soil-pile-structure interaction on full-scale piled rafts have been reported (Yamashita et al., 2012; Yamashita et al., 2016). It has become necessary to develop more reliable design methods for piled rafts which could predict the settlement behaviour more accurately. It is now well recognized that the settlement of a pile group can differ significantly from that of a single pile at the same average load level due to the effects of group interaction, i.e., the mutual interactions of the piles within the pile group (Poulos and Davis, 1980; Randolph, 1994; Mandolini et al., 2005; Poulos, 2012). Cooke et al. (1981) reported a case history of a friction piled raft supporting 16-story apartment, where settlement of the piled raft was compared with that from vertical pile load testing of a single pile. Mandolini and Viggiani (1997) proposed an analytical method for estimating load-settlement behaviour of piled rafts, considering interactions between pile group and raft based on elastic method where initial stiffness of a single pile obtained from load testing is used. However, not so many case histories exist on examining the effects of pile group interaction. Hence, it is required to investigate the effects of group interaction in full-scale piled rafts to allow more accurate settlement prediction. In this paper, the effects of group interaction were investigated based on the monitoring data for the piles in two piled rafts and the results of single pile load tests. In addition, the rate effects with rapid load pile testing in clay soils were examined in comparison with the static load test result.

2. CASE HISTORIES

Two case histories in soft ground are presented from which load-settlement data of the piles were derived; one of a piled raft consisting of piles embedded in very dense sand with large spacing supporting a 12-story building, and the other of a piled raft consisting of friction piles with large spacing supporting a 7-story building. The 12-story building is located in Tokyo about 300 m away from the 7-story building as shown in Figure 1, and the soil conditions in the two sites are quite similar. Since the rafts of both the buildings were embedded in loose sand underlain by soft clay soils, in order to enhance bearing capacity of the rafts as well as a countermeasure of liquefaction below the rafts induced by large earthquakes, piled raft foundation combined with grid-form cement deep mixing walls (DMWs) was employed (Yamashita et al., 2011b; Yamashita et al., 2013).

At the foundation design stage, in order to verify the design bearing capacity of the piles, static load test and rapid load pile testing (RLT) of single piles were carried out in both the sites. In addition, to confirm the validity of the foundation design, long-term field monitoring was performed on the foundation settlements, axial loads of the piles and contact pressure beneath the raft.

On March 11, 2011, the 2011 off the Pacific coast of Tohoku Earthquake (the 2011 Tohoku earthquake), with an estimated magnitude of M_w= 9.0 on the Moment Magnitude Scale, struck East Japan. The distance from the epicentre to the building sites was about 380 km, and the monitoring results of the piled rafts before and after the event were successfully obtained.

Figure 1 Locations of 12-story and 7-story buildings

2.1 Twelve-story Office Building

2.1.1 Building and foundation

The 12-story office building is a steel-framed structure with a base isolation system of laminated rubber bearings that was completed in 2011 (Figure 2). Figure 3 illustrates a schematic view of the structure and foundation with a soil profile. The average contact pressure over the raft was 187 kPa. Thus, the piled raft consisted of 180 PHC (pretensioned spun high strength concrete) piles of 0.6 to

1.2 m in diameter where nominal compressive strength of concrete was 105 N/mm^2. The pile toes were embedded in the thick very dense sand layers below a depth of 44 m. The pile was constructed by inserting the precast piles into a pre-augered borehole filled with mixed-in-place soil cement for shaft and with concrete for foot protection in order to enhance the toe resistance. Figure 4 illustrates the foundation plan with the locations of the monitoring devices. The center-to center spacing of the piles was relatively large, 8-12 times the diameter in the tributary area. More details such as foundation design and instrumentation were given in a previous paper (Yamashita et al., 2013).

2.1.2 Static load test of single pile

Static compression load test of a single pile was carried out to verify the design bearing capacity. Figure 5 illustrates the test pile together with the monitored piles P1-P4. The test pile and the monitored piles have similar length, but different diameter, i.e., the test pile is 0.6 m in diameter while the monitored piles are 1.2 and 0.8 m. The test pile was located near the south end of the foundation as shown in Figure 4.

Figure 2 View of 12-story office building

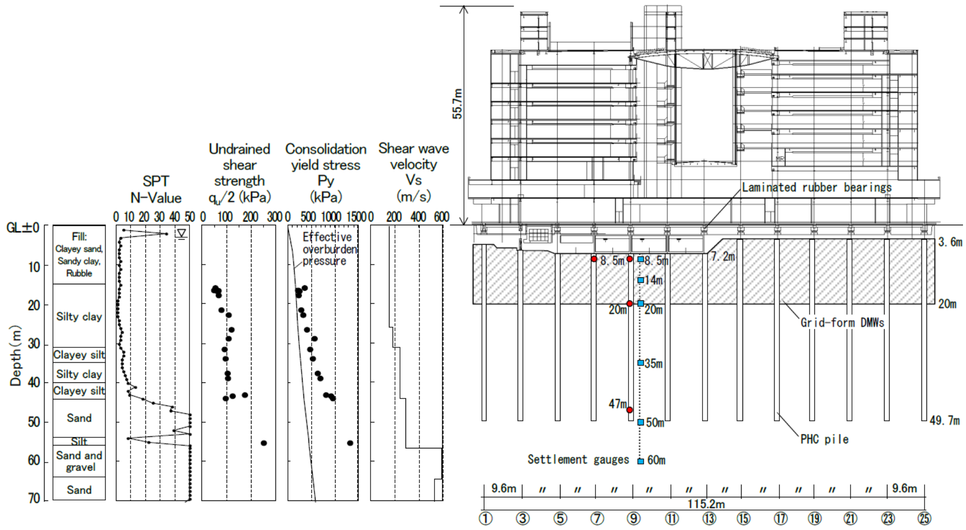

Figure 3 Schematic view of 12-story building and foundation with soil profile

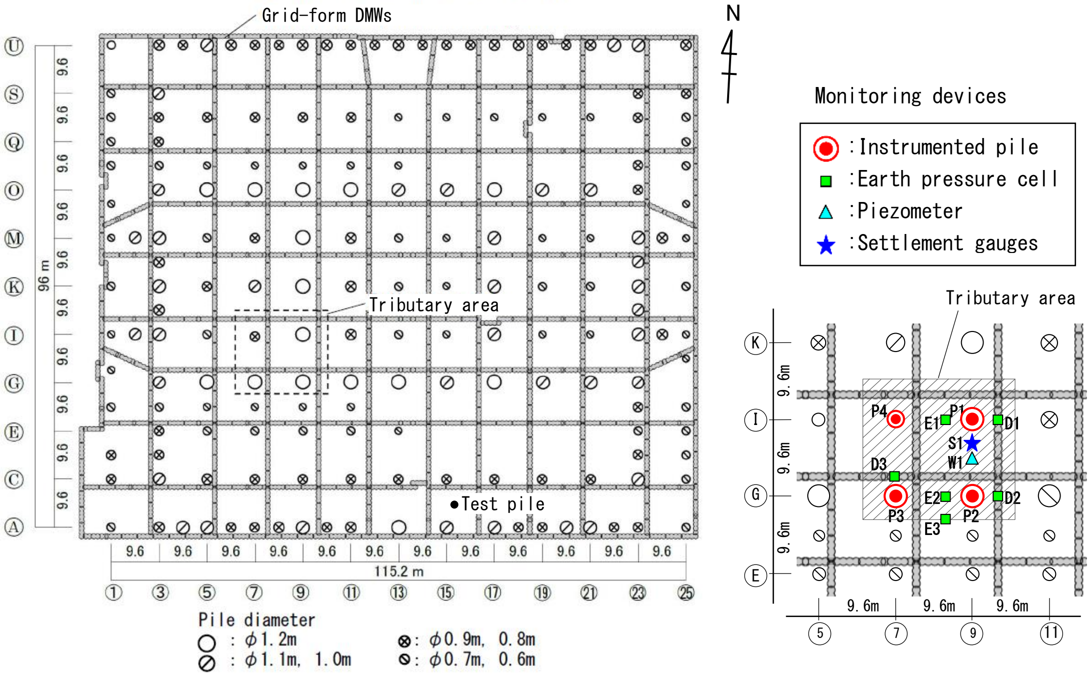

(a) Layout of piles and grid-form cement deep mixing walls (b) Locations of monitoring devices

Figure 4 Foundation plan with locations of monitoring devices

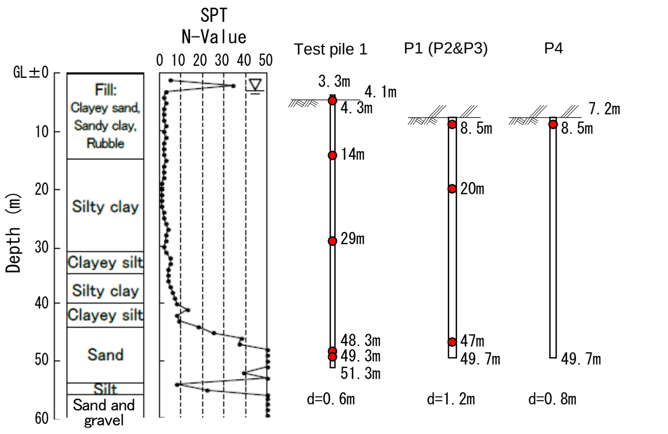

Figure 5 Test pile 1 and monitored piles P1-P4

Figure 6 illustrates a setup for the pile load test. There were four anchor piles which were located larger than 3.3 diameters from the test pile. The load testing was conducted 27 days after the construction of the test pile, and had five load cycles with a maximum load of 9.44 MN.

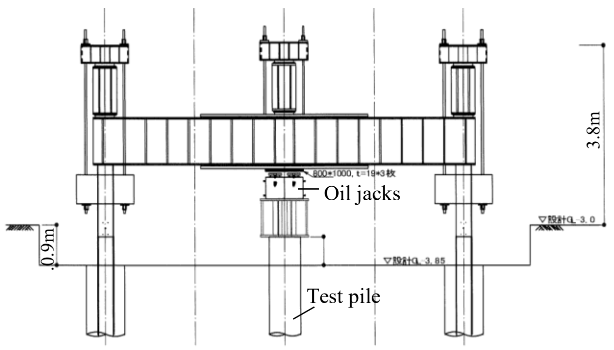

Figure 6 Setup for compression load test

Figure 7 shows the load-settlement curves at the pile head obtained from the static pile load testing. Under the maximum load, the pile head settlement was 63.8 mm which corresponds to about 11% of the pile diameter.

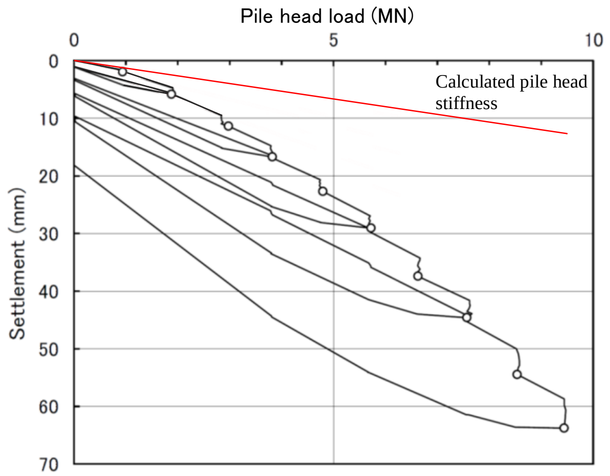

Figure 7 Load-settlement curve at pile head from SLT with calculated pile head stiffness

2.1.3 Results of monitoring piles

Field monitoring was performed from the beginning of the construction to 58 months after the end of the construction (E.O.C.). Figure 8 shows the measured vertical ground displacements below the raft versus time. The ground displacement at a depth of 8.5 m after the casting of raft was approximately equal to the settlement of the raft, and refers to raft settlement in this paper. At the time of the 2011 Tohoku earthquake, nine months before E.O.C. about 80 % of the total structure load acted on the foundation. The raft settlement was 15.0 mm on March 1, 2011, before the earthquake, and increased by 0.8 mm from the pre-earthquake value to 15.8 mm on March 16, 2011. Thus, no significant change in raft settlement was observed after the event. Thereafter, the settlement became stable and reached 21 mm at the end of the observation.

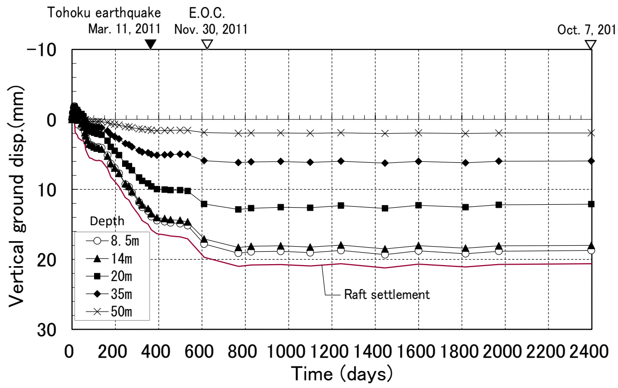

Figure 8 Measured vertical ground displacements below raft

Figure 9 shows the development of the measured axial loads of four piles (P1-P4) versus time. The axial loads became stable after E.O.C. in a same way as the raft settlement. Figure 10 shows the measured axial loads along Pile P1 versus time. The average shaft friction between the depths of 8.5 and 20.0 m was quite small, and about 80% of the pile head load was carried by the shaft friction after E.O.C. Figure 11 shows the development of the measured contact pressure between the raft and the soil and that between the raft and the DMWs, together with the porewater pressure beneath the raft.

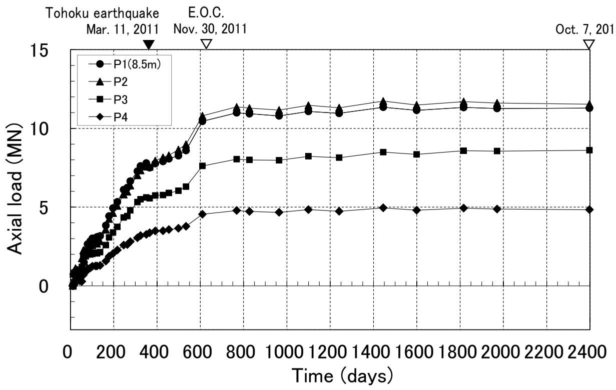

Figure 9 Measured pile head axial loads

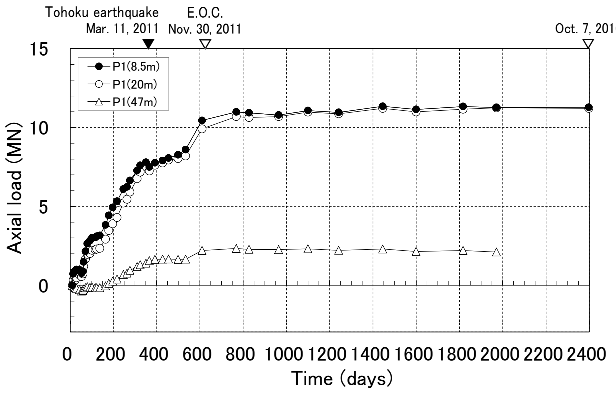

Figure 10 Measured axial loads of Pile P1

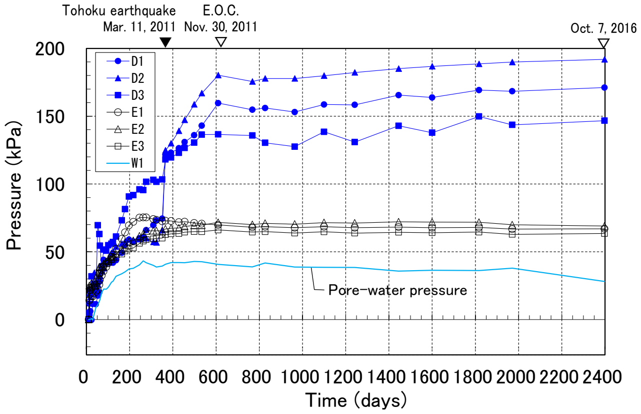

Figure 11 Measured contact pressure and porewater pressure

Figure 12 shows the time-dependent load sharing among the piles, the soil, the DMWs and the buoyancy in the tributary area of the instrumented piles. After E.O.C., the load sharing among the piles, the DMWs and the soil was quite stable. The ratios of the load carried by the piles to the net load (the gross structure load minus the buoyancy) were estimated to be 0.66-0.71 after E.O.C., while the ratio of the net load carried by the soil to the net structure load and that carried by the DMWs were around 0.15.

2.1.4 Load-settlement data of piles derived from monitoring

Figure 13 shows the relationships between the pile head load and the pile head settlement of the monitored piles P1-P4. The relationships were obtained using the settlement vs. time and the pile head load vs. time data shown in Figures 8 and 9, respectively. The pile head settlement means vertical ground displacement (measured near the instrumented piles) at the depth of 7.2 m after casting of the raft, which was obtained by extrapolating the ground displacements at the depths of 8.5 and 14.0 m. It is seen that the pile head load increased almost linearly with the increase in pile head settlement. At the time of the 2011 earthquake, hysteretic load-unload vs. settlement relationship can be seen on the load-settlement data of Piles P1-P3. This may have been caused by the vertical cyclic loading during the event.

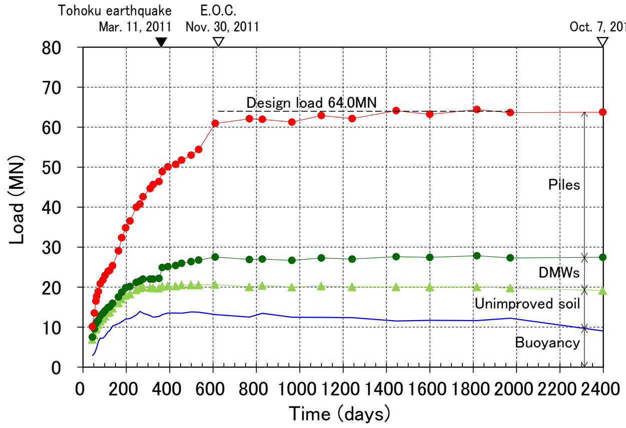

Figure 12 Load sharing among piles, DMWs and soil in the tributary area

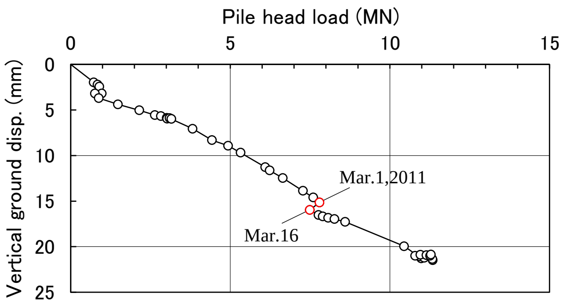

(a) Pile P1 (d=1.2m)

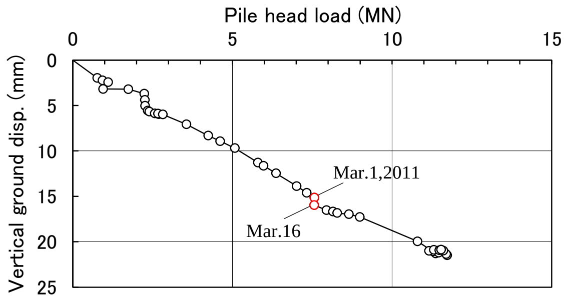

(b) Pile P2 (d=1.2m)

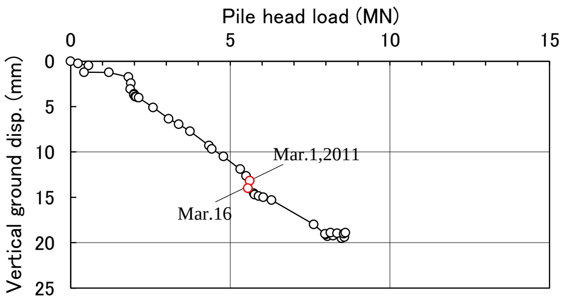

(c) Pile P3 (d=1.2m)

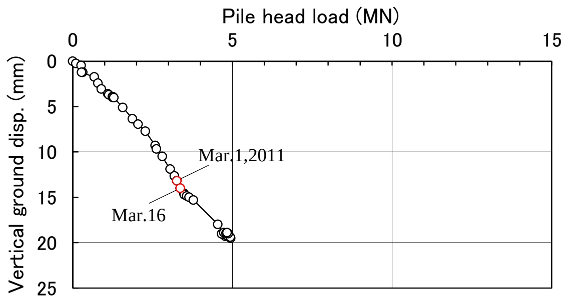

(d) Pile P4 (d=0.8m)

Figure 13 Load-settlement data at pile head derived from field monitoring

Figure 14 shows the load-settlement data of the monitored piles together with the load test result. It is seen that the pile head stiffness, which means pile head load (P) devided by the pile head settlement (w) of the monitored piles (1.2 and 0.8 m in diameter) was larger than that of the test pile (0.6 m in diameter). Hence, considering the slender piles with similar length of different diameter, the P/d vs. w relationships for the test pile and the monitored piles are shown in Figure 15. It is seen that the load-settlement relationships of the monitored piles were roughly consistent with that of the test pile. This suggests that pile group effect on settlement was not significant in this case.

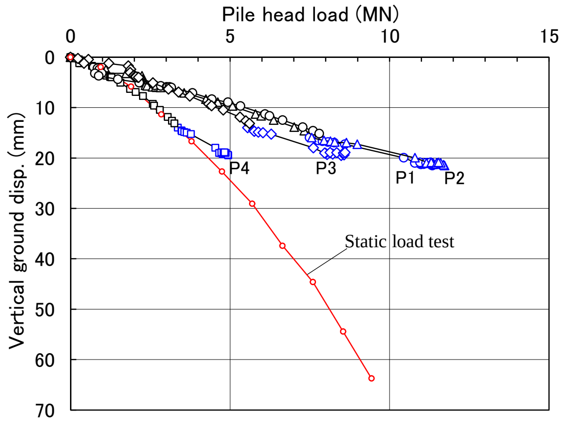

Figure 14 Load-settlement curves from field monitoring and SLT

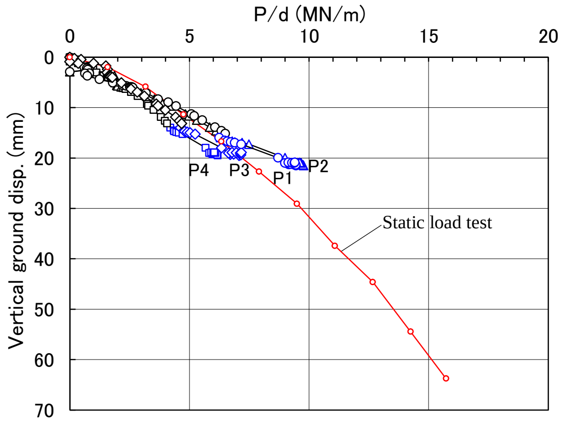

Figure 15 *P*/*d* vs. *w* relationship derived from monitoring and static load test

2.2 Seven-story Office Building

2.2.1 Building and foundation

The 7-story office building is a steel-frame structure that was completed in 2004 (Figure 16). Figure 17 illustrates a schematic view of the structure and foundation with a soil profile. A total load in the structural design was 378 MN which corresponds to the sum of the dead load and the live load of the building. The average contact pressure over the raft was 100 kPa. The foundation level was at a depth of 2.2 m in the central part and at a depth of 1.6 m in the north and south ends. In order to reduce the average and differential settlement due to consolidation of the very soft silt layers to an acceptable level, seventy friction piles were employed as settlement reducers. The piles are 30 m long, 0.6 to 0.9 m in diameter, PHC piles. Figure 18 illustrates the layout of the piles and the grid-form DMWs. The typical pile spacing was 12-18 times the diameter. Further details such as foundation design and instrumentation were described in a previous paper (Yamashita et al., 2011b; Yamashita et al., 2016).

Figure 16 View of 7-story building

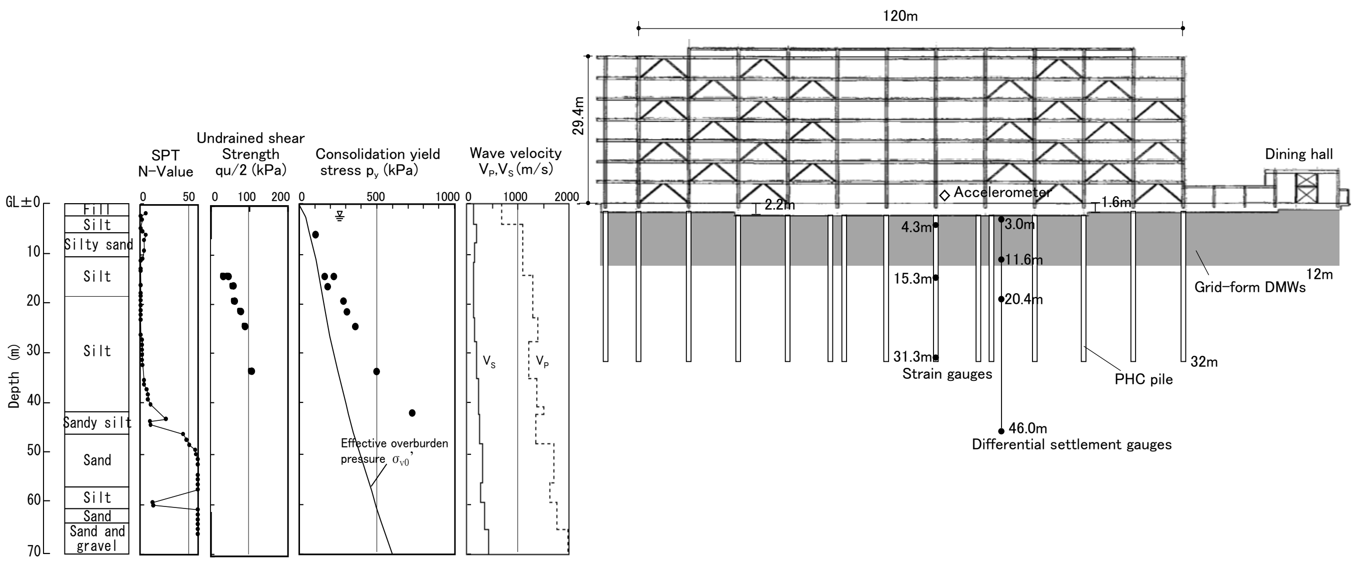

Figure 17 Schematic view of 7-story building and foundation with soil profile

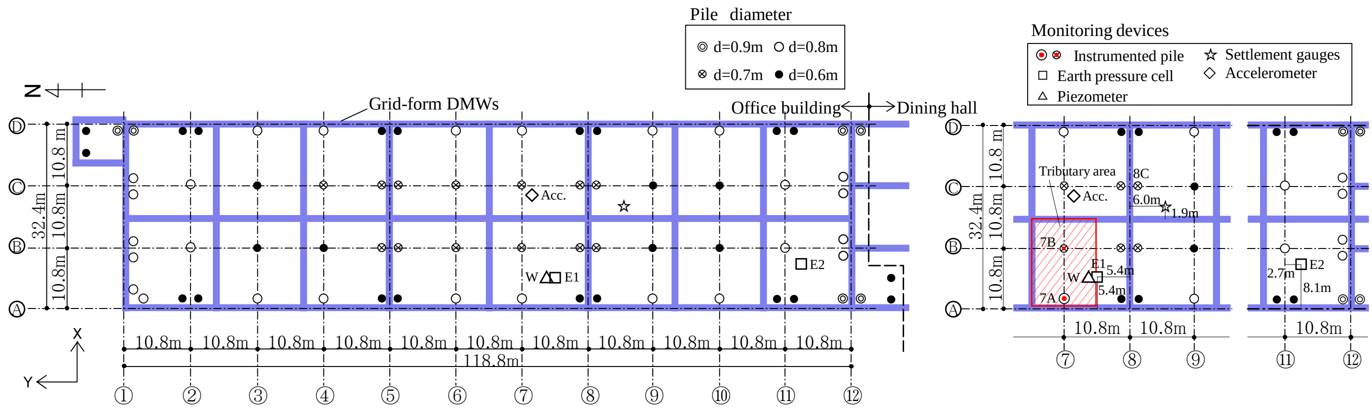

(a) Layout of piles and grid-form DMWs

(b) Locations of monitoring devices

Figure 18 Foundation plan with locations of monitoring devices

2.2.2 Rapid load pile testing

A pile load test was conducted using a falling mass type rapid load pile testing (RLT) technique (Matsumoto et al., 2007; Yamashita, 2015). This method utilises a falling mass and soft cushion on the pile top to prolong loading duration as shown in Figure 19.

Figure 19 Falling mass type rapid load pile testing

Figure 20 illustrates the test pile together with the monitored piles 7A and 7B. The test pile was 0.8 m in diameter and 32.0 m in embedded length and was located near the south end of the building. The load testing was conducted 31 days after the construction of the pile, and had eight load cycles. The hammer mass was 32.9 tons and the load cycles of the pile testing with falling height of the mass are shown in Table 1. The load signals on the pile top was measured by a load cell, and the vertical displacement and acceleration at the pile head were measured by an optical displacement transducer and an accelerometer, respectively.

Figure 21 shows the load and vertical displacement signals at the pile head in the 8th load cycle of the maximum falling height. The maximum load and displacement at the pile head were 10.51 MN and 23.8 mm, respectively. Figure 22 shows the load-settlement curves recorded in each load cycle, together with the equivalent static curve derived from the unloading point method (UPM) (Middendorp et al., 1993). In rapid load pile testing, the relatively long loading duration allows the pile to be modelled as a mass on which rapid load on the pile top, inertial force of the pile and soil resistance (sum of static soil resistance and damping force from soil) are acting. The UPM assumes that the pile resistance at the unloading point where the pile has zero velocity is equivalent to the static pile resistance if the inertial forces are negligible.

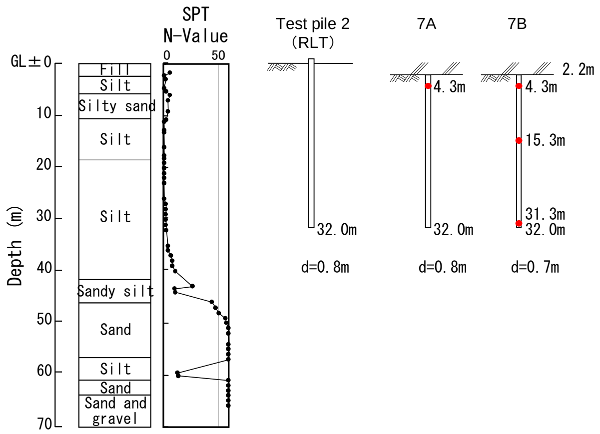

Figure 20 Test pile 2 and monitored piles 7A and 7B

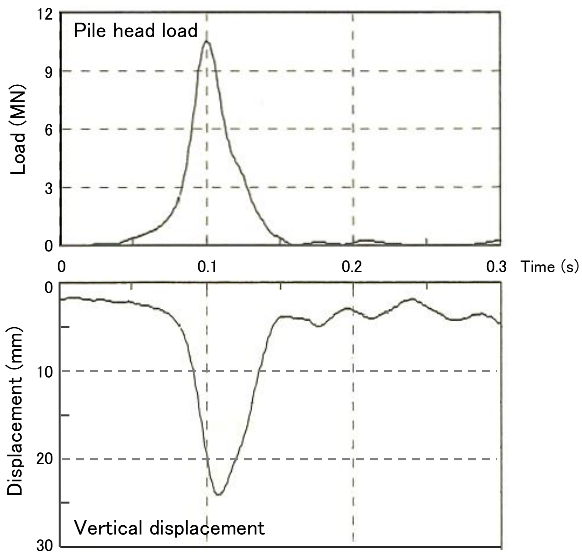

Figure 21 Load and displacement signals at pile head (8th cycle)

Table 1 Load cycles

Cycle	Falling height (m)
1	0.20
2	0.44
3	0.64
4	0.83
5	1.04
6	1.23
7	1.43
8	1.64

2.2.3 Results of monitoring piles

Field monitoring was performed from the beginning of the construction to 125 months after E.O.C. Figure 23 shows the development of the measured vertical ground displacement below the raft. The vertical ground displacement at a depth of 3.0 m after the casting of raft refers to raft settlement. The raft settlement reached 22.3 mm on March 10, 2011, just before the 2011 Tohoku earthquake. On March 15, 2011, the raft settlement increased by 1.1 mm to 23.4 mm. Thereafter, the settlement became stable.

Figure 24 shows the development of the measured axial loads of Pile 7B. The measured pile head axial load reached 5.62 MN on Pile 7B on March 10, 2011.

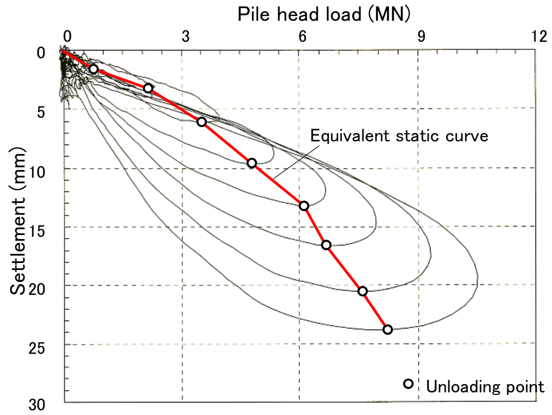

Figure 22 Rapid load-settlement curves and equivalent static load-settlement curve

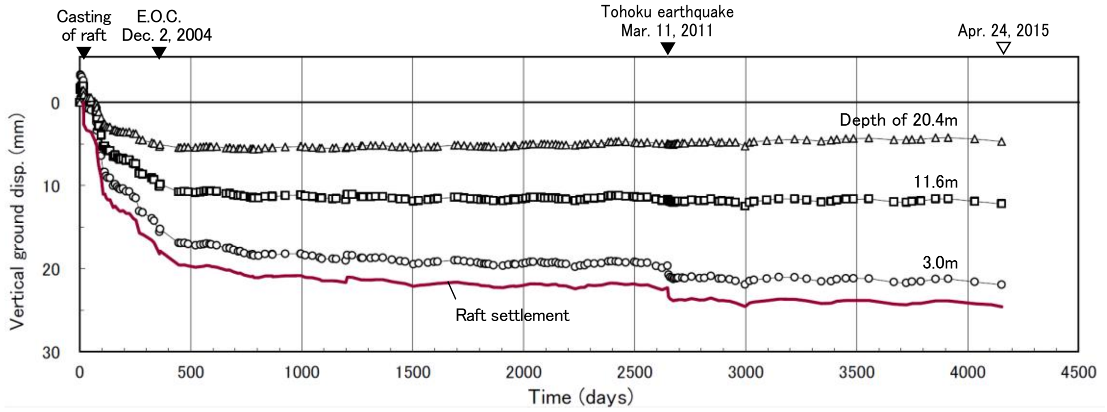

Figure 23 Measured vertical ground displacements vs. time

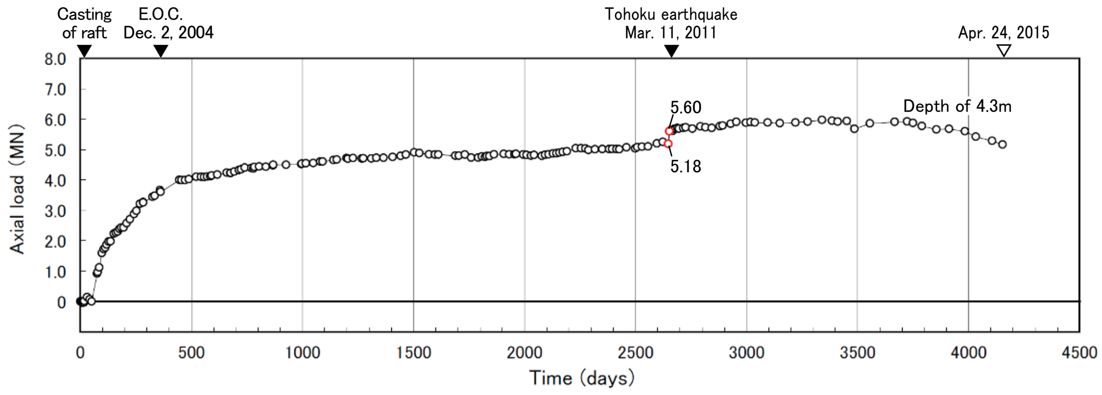

(a) Pile 7A

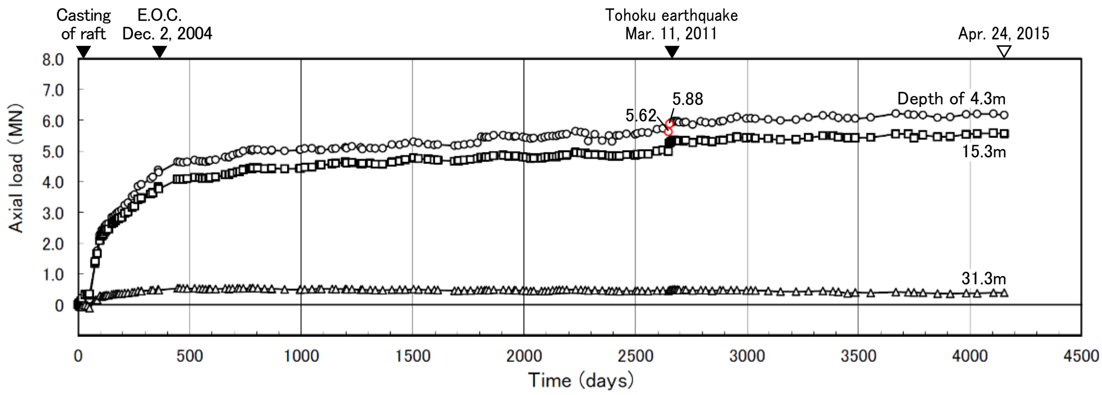

(b) Pile 7B

Figure 24 Measured axial load of Pile 7B vs. time

On March 15, 2011, the pile head load of Pile 7B increased by 0.26 MN to 5.88 MN. Figure 24(b) indicates that the increment in pile head load was compensated almost entirely by the increment in lower shaft resistance between the depths of 15.3 and 31.3 m. Thereafter, the pile head axial load of Pile 7A increased slightly and then turned to decrease, while the axial loads of Pile B near the pile head and the intermediate depth increased very slightly and became stable.

Figure 25 shows the measured contact pressure between the raft and the unimproved soil together with the pore-water pressure beneath the raft versus time. After the earthquake, no significant changes in contact pressure from both of E1 and E2 were observed.

Figure 26 shows the development of the load carried by the piles and the unimproved soil in the tributary area. The ratio of the load carried by the piles to the net structure load was estimated to be 0.75 at the end of the observation, while the load carried by the piles showed some increase at the time of the earthquake.

2.2.4 Load-settlement data of piles derived from monitoring

Figure 27 shows the relationship between the pile head load of the monitored piles 7A and 7B and the pile head settlement. These relationships were obtained from the data shown in Figures 23 and 24. The pile head settlement means vertical ground displacement at the depth of 2.2 m after casting of the raft, which was obtained by extrapolating the ground displacements at the depths of 3.0 and 11.6 m. Although Piles 7A and 7B were located 18-23 m away from the ground displacement measuring point as illustrated in Figure 18, the difference of settlement between the column 7A and the displacement measuring point was found to be negligible (less than 2 mm after E.O.C.) according to the optical level measurement. It is seen that the pile head load increased almost linearly with the increase in pile head settlement, as in the case of the 12-story building (Figure 13).

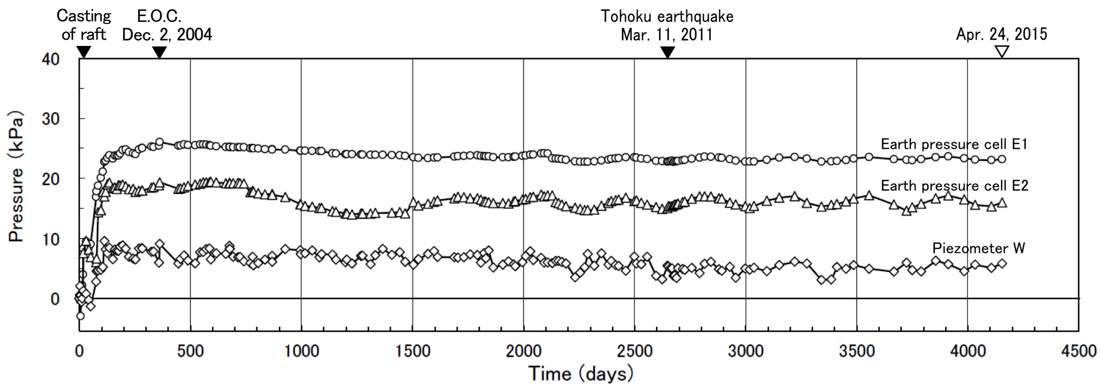

Figure 25 Measured contact pressure and pore-water pressure vs. time

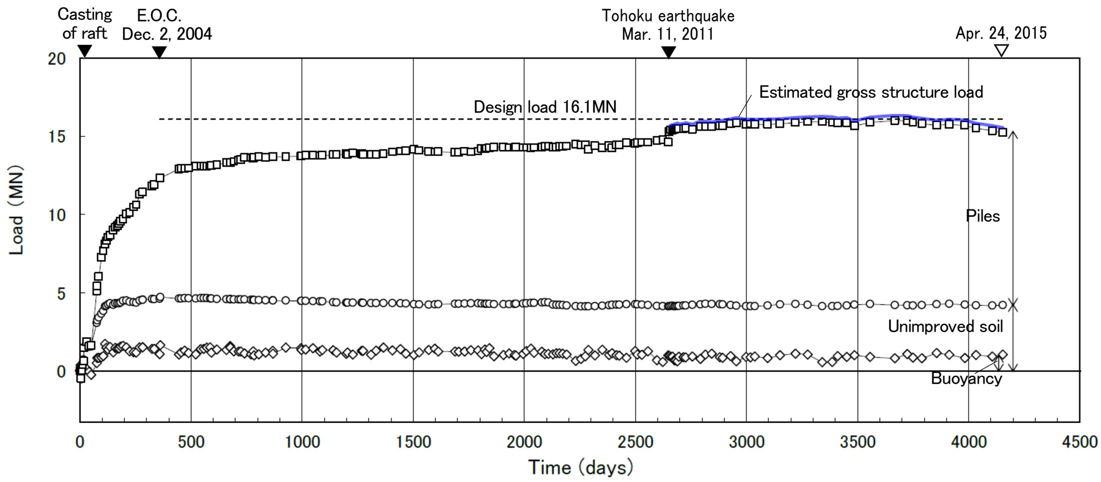

Figure 26 Development of loads carried by piles and unimproved soil in tributary area

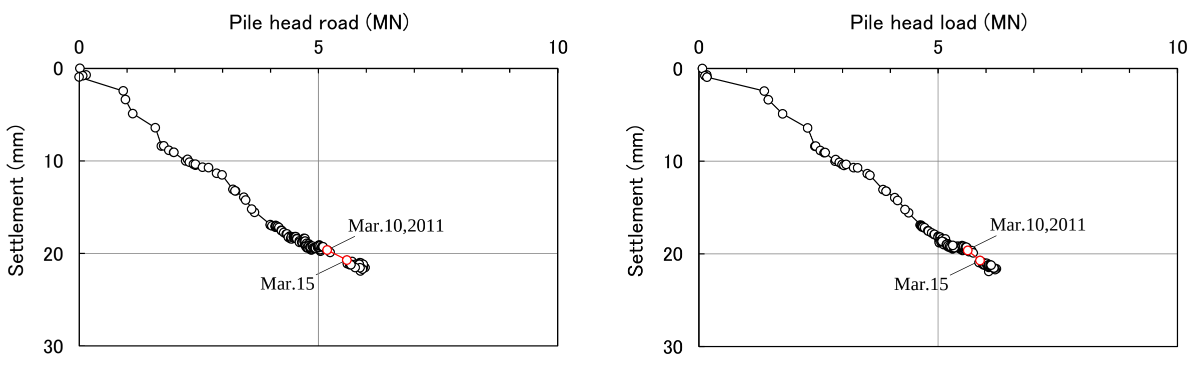

(a) Pile 7A

(b) Pile 7B

Figure 27 Load-settlement data at the pile head derived from field monitoring

Figure 28 shows the P/d vs. w relationships obtained from the equivalent static load-settlement curve (RLT) and the load-settlement data of the monitored piles, considering the piles with similar length of different diameter. The stiffness of the P/d vs. w relationship of the test pile is somewhat higher than that of the monitored piles. It would seem that the former was overpredicted due to the rate effects with RLT in clay soils, and/or the latter was reduced by the effects of group interaction. Further discussion is made in the following section.

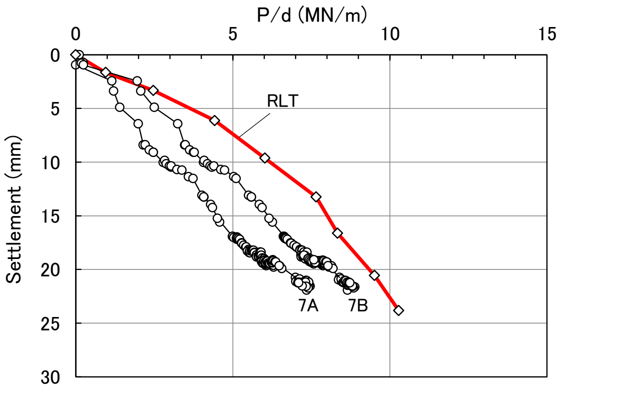

Figure 28 Pt/d vs. w relationship derived from monitoring and RLT

3. DISCUSSION OF MONITORING AND TEST RESULTS

3.1 Effects of Pile Group Interaction

The effects of group interaction on the load-settlement data of the monitored piles were examined in comparison with the static load test result of a single pile. In order to compare the pile head stiffness of different dimensions (diameter, cross section and length), the dimensions of the monitored piles were adjusted to those of Test pile 1 by means of an approximate approach using a modification factor. The modification factor means the ratio of the pile head stiffness of Test pile 1 to that of the other piles, considering the static load-settlement curve of Test pile 1 as a benchmark. The modification factor may be obtained using pile head stiffness k ($=P/w$) derived from an elastic solution for the axial response of a single pile (Randolph and Wroth, 1978).

Figure 29 illustrates profiles of the test and monitored piles with soil shear modulus at small strain, G_0, in an analytical model. Although pile-top depths of the test and monitored piles were different, they were assumed to be identical to the ground surface level for simplicity. The soil shear modulus indicated by a red line was assumed based on the shear wave velocity derived from the P-S logging shown in Figures 3 and 17.

The dimensions of the piles and the soil properties in the analytical model are shown in Table 2. While the Young's modulus of the PHC pile is 40000 MPa (nominal value), the pile was considered as solid with Young's modulus, E_p, such that the cross-sectional rigidity is equivalent to that of the original hollow pile. Table 2 also shows the calculated initial pile head stiffness and modification factors. It should be noted that the modification factor, k_{T1}/k_{P123} (stiffness ratio of Test pile 1 to Piles P1-P3) or k_{T1}/k_{P4} (stiffness ratio of Test pile 1 to Pile P4), was found to be close to the ratio of the pile diameter, as is expected for slender piles. To confirm the validity of the analysis, the calculated pile head stiffness of Test pile 1 was compared with the static load-settlement curve shown in Figure 7. It was found that the initial pile head stiffness was consistent with that of the load-settlement curve.

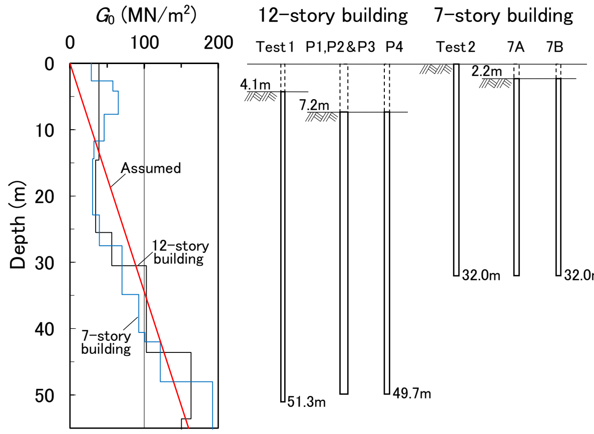

Figure 29 Soil shear modulus with test and monitored piles in analytical model

$$\frac{P}{w\,dG_{L_p}}=\frac{\dfrac{2}{(1-\nu_s)\xi}+\dfrac{2\pi\rho}{\zeta}\dfrac{\tanh(\mu L_p)}{\mu L_p}\dfrac{L_p}{d}}{1+\dfrac{8}{\pi\lambda(1-\nu_s)\xi}\dfrac{\tanh(\mu L_p)}{\mu L_p}\dfrac{L_p}{d}} \qquad (1)$$

where

- P: pile-head load
- w: pile-head settlement
- L_p: pile length
- d: pile diameter
- G_{ave}: average shear modulus of soil along pile length
- G_{Lp}: shear modulus of soil at a depth of pile length
- G_b: shear modulus of soil below the level of pile base
- ν_s: Poisson's ratio of soil
- r_m: maximum radius of influence of pile
- $\xi = G_{Lp}/G_b$
- $\rho = G_{ave}/G_{Lp}$
- $\lambda = E_p/G_{Lp}$
- $\zeta = \ln(2r_m/d)$
- $\mu L_p = 2\sqrt{2/\zeta\lambda}\,(L_p/d)$

Table 2 Initial pile head stiffness and modification factors with dimensions of piles and soil properties

		Pile				Soil			Pile head stiffness k (MN/m)	Modification factor k_{T1}/k
		d (m)	L_P (m)	A_P (m^2)	E_P (MPa)	G_{Lp} (MPa)	ρ	ν_s		
12-story building	Test pile 1	0.6	51.3	0.195	27600	149	0.5	0.3	k_{T1} = 710	1.0
	Monitored piles P1,P2,P3 P4	1.2 0.8	49.7	0.633 0.266	22400 21200	145	0.5	0.3	k_{P123}=1363 k_{P4}= 853	0.52 (0.50)※ 0.83 (0.75)※
7-story building	Test pile 2	0.8	32.0	0.249	19800	93	0.5	0.3	k_{T2} = 675	1.05
	Monitored piles 7A 7B	0.8 0.7	32.0	0.249 0.197	19800 20500	93	0.5	0.3	k_{7A} = 675 k_{7B} = 592	1.05 1.20

※ Value in parentheses indicates pile diameter ratio

The load-settlement data of the monitored piles were modified by multiplying the modification factor to the pile head load in the load-settlement data. Figure 30 shows the modified load-settlement data of all the monitored piles together with the static load test curve of Test pile 1. It is seen that the pile head stiffness of Pile 7A as well as that of Pile P1-P4 are generally consistent with, or slightly larger than, that of the single pile, while the pile head stiffness of Pile 7B is somewhat larger than the others.

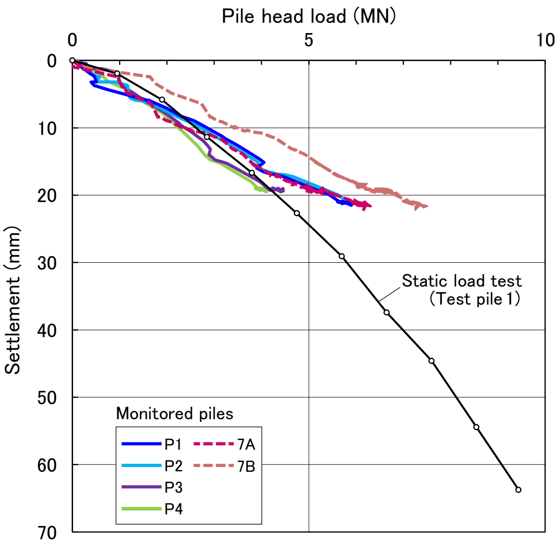

Figure 30 Comparison of modified load-settlement data of monitored piles with static load test curve of Test pile 1

In general, the stiffness of each pile in a group is reduced in comparison with that of a single pile at the same average load level due to the effects of group interaction. Cooke et al. (1981) have presented a case history of a friction piled raft supporting 16-story apartment on London clay, where settlement of the piled raft was compared with that from pile load test to examine the effects of group interaction. The piled raft consisted of 351 friction piles (0.45 m in diameter and 13 m long, and the center-to-center pile spacing was 3.6 diameters). Based on the field monitoring results, the settlement ratio, which is originally defined as the ratio of the flexibility of a pile in the group to that of an isolated pile (Poulos and Davis, 1980), was found to be about nine at the building operation, and increased to 16 four years after the building operation.

In contrast to the case history presented by Cook et al. (1981), no significant pile group effect on settlement was observed in the two cases described in this paper. This may have arisen because the ratio of the pile spacing to the pile diameter (pile spacing ratio) was relatively large, larger than about eight, where the effects of group interaction seemed to be negligible. Mandolini et al. (2005) pointed out based on the experimental evidence by the monitoring of full-scale structures that the pile spacing ratio plays a major role in load sharing between the raft and the piles. Yamashita et al. (2011a) presented that although the ratio of the load carried by the piles to the net structure load decreases as the pile spacing ratio increases, the ratio tends to become constant at the pile spacing ratio greater than about six. Thus, the results described in this paper are consistent with those described by Mandolini et al. (2005) and Yamashita et al. (2011a). In addition, it is likely that the head stiffness of actual piles became larger than that of test piles because the strength of clay soils surrounding the piles was increased due to consolidation during the long monitoring period.

3.2 Rate Effects with RLT in Clay Soils

In order to examine the rate effect on load-settlement behaviour of piles subjected to rapid loading, Figure 31 compares the estimated equivalent static curve of Test pile 1 with the static load test curve of Test pile 1. The equivalent static behaviour was obtained by multiplying the modification factor to the pile head load in the equivalent static curve of Test pile 2. The modification factor of 1.05 was resulted in offsetting the effect of diameter against that of length on the pile head stiffness. It was found that the pile head stiffness of the estimated equivalent static curve was considerably larger than that of the static load-settlement curve.

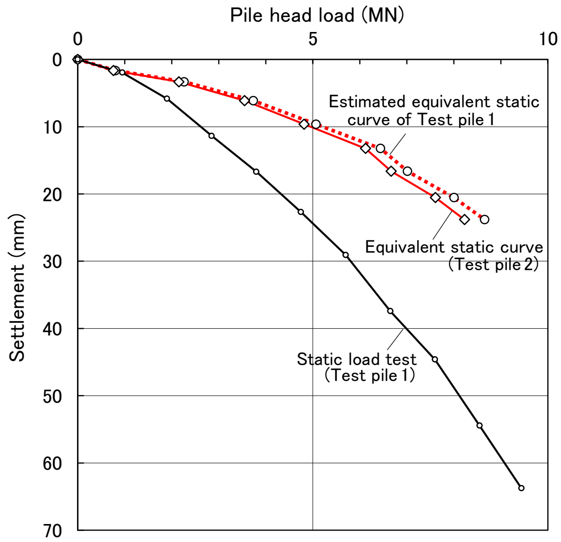

Figure 31 Comparison of estimated equivalent static curve of Test pile 1 with static load test curve of Test pile 1

The ratio of the pile head stiffness from the static load test to that from the RLT versus the pile head load is shown in Figure 32. The ratio is varied from 0.50 to 0.57 for the range of $w/d< 0.03$ except for one at the initial loading. Namely, the pile head stiffness derived from the RLT was about two times the stiffness of the static load-settlement curve.

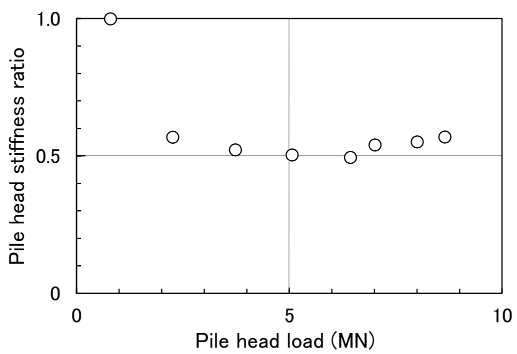

Figure 32 Pile head stiffness ratio (Static test/ RLT)

Brown et al. (2013) pointed out that the equivalent static load-settlement behaviour derived from the UPM did not adequately describe the rate effects in clays and silts, with overprediction of ultimate capacity although good performance was noted where piles were installed in coarse-grained soils. The results described in this paper are consistent with the study by Brown et al. (2013).

4. CONCLUSIONS

The effects of group interaction on the load-settlement behaviour of piles were investigated based on the results of two monitoring cases of piled raft foundations, where 70-80% of the structure load was carried by the piles, and the single pile load tests. In addition, the rate effects with rapid load pile testing in clay soils were examined in comparison with the static load test result. Through the investigation, the following conclusions can be drawn:

1) By considering the effect of different pile dimensions on the pile head stiffness using a modification factor derived from elastic solution for the axial response of a single pile, it was found that the modified load-settlement data of the monitored piles were generally consistent with the static load-settlement curve of a single pile. Therefore, no significant effects of group interaction on settlement were found for the piles with large spacing (larger than about eight times the diameter) in piled raft system. In such cases, single pile load test data can be more useful in the prediction of settlement of piled rafts and pile groups.
2) The rate effect on the load-settlement behaviour of piles in clay soils subjected to rapid loading was notably seen. It was found that the pile head stiffness of the equivalent static curve derived using the UPM was about two times the stiffness of the static load-settlement curve.

5. ACKNOWLEDGEMENTS

The authors are grateful to Prof. T. Matsumoto of Kanazawa University for his useful discussions and constructive comments. The authors are also grateful to Messrs. A. Miyashita, H. Matsuzaki, H. Nagaoka of Takenaka Corporation for their contribution to the foundation design.

6. REFERENCES

Brown, M. J. and Powell, J. J. M. (2013) “Comparison of Rapid Load Test Analysis Techniques in Clay Soils”, Journal of Geotechnical and Geoenvironmental Engineering, ASCE, Vol. 139, No. 1, pp152-161.

Cooke, R. W., Bryden-Smith, D. W., Gooch, M. N. and Sillet, D. F. (1981) ”Some observations of the foundation loading and settlement of a multi-storey building on a piled raft foundation in London Clay”, Proc. Instn Civ. Engrs, Part 1, Vol.70, pp433-460.

Katzenbach, R., Arslan, U. and Moormann, C. (2000) “Piled raft foundation projects in Germany”, Design applications of raft foundations, Hemsley J.A. Editor, Thomas Telford, pp323-392.

Mandolini, A. and Viggiani, C. (1997) “Settlement of piled foundations”, Geotechnique, 47(4), pp791-816.

Mandolini, A., Russo, G. and Viggiani, C. (2005) “Pile foundations: Experimental investigations, analysis and design”, Proc. of the 16th Int. Conference on SMGE, Vol. 1, pp177-213.

Matsumoto, T., Kitiyodom, P. and Shintani, T. (2007) “Trend of research and practice of pile foundations in Japan, Proc. of Int. Workshop on Recent Advances in Deep Foundations”, pp143-173.

Middendorp, P. (1993) “First experiences with Statnamic load testing of foundation piles in Europe”, Proc. of the 2nd International Geotechnical Seminar on Deep Foundations and Auger Piles, BAP II, pp265-272.

Poulos, H.G. and Davis, E.H. (1980) Pile Foundation Analysis and Design, John Wiley and Sons.

Poulos, H.G. (2012) “Pile testing and settlement prediction”, Full-scale Testing and Foundation Design, GeoCongress 2012, pp630-649.

Randolph, M.F. and Wroth, C.P. (1978) “Analysis of deformation of vertically loaded piles”, Jnl. Geot. Eng., ASCE, 104(GT12) pp1465-1488.

Randolph, M.F. (1994) “Design methods for pile groups and piled rafts”, Proc. of the 13th Int. Conference on SMFE, pp61-82.

Yamashita, K., Yamada, T. and Hamada, J. (2011a) “Investigation of settlement and load sharing on piled rafts by monitoring full-scale structures”, Soils & Foundations, Vol. 51, No. 3, pp513-532.

Yamashita, K., Hamada, J. and Yamada, T. (2011b) “Field measurements on piled rafts with grid-form deep mixing walls on soft ground”, Geotechnical Engineering Journal of the SEAGS & AGSSEA, Vol. 42, No. 2, pp1-10.

Yamashita, K., Hamada, J., Onimaru, S. and Higashino, M. (2012) “Seismic behavior of piled raft with ground improvement supporting a base-isolated building on soft ground in Tokyo”, Soils & Foundations, Vol. 52, No. 5, pp1000-1015.

Yamashita, K., Wakai, S. and Hamada, J. (2013) “Large-scale piled raft with grid-form deep mixing walls on soft ground”, Proc. of the 18th Int. Conference on SMGE, pp2637-2640.

Yamashita, K. (2015) “Settlement of piled raft subjected to strong seismic motion”, 15th Asian Regional Conference on SMGE, JPN-87.

Yamashita, K., Hamada, J. and Tanikawa, T. (2016) “Static and seismic performance of a friction piled combined with grid-form deep mixing walls in soft ground”, Soils & Foundations, Vol. 56, No. 3, pp559-573.